# Simultaneous Electropolymerization and Electro-Click Functionalization for Highly Versatile Surface Platforms

Gaulthier Rydzek,[†,*] Tatyana G. Terentyeva,[†] Amir Pakdel,[†] Dmitri Golberg,[†] Jonathan P. Hill,[†,‡] and Katsuhiko Ariga[†,‡,*]

[†]World Premier International (WPI) Research Center for Materials Nanoarchitectonics (MANA), National Institute for Materials Science (NIMS), 1-1 Namiki, Tsukuba 305-0044, Japan and [‡]Core Research for Evolutional Science and Technology (CREST), Japan Science and Technology Agency (JST), 1-1 Namiki, Tsukuba 305-0044 Japan

ABSTRACT Simple preparation methods of chemically versatile and highly functionalizable surfaces remain rare and present a challenging research objective. Here, we demonstrate a simultaneous electropolymerization and electro-click functionalization process (SEEC) for one-pot self-construction of aniline- and naphthalene-based functional polymer films where both polymerization and click functionalization are triggered by applying electrochemical stimuli. Cyclic voltammetry (CV) can be applied for the simultaneous oxidation of 4-azidoaniline and the reduction of Cu(II) ions, resulting in

polymerization of the former, and the Cu(I)-catalyzed alkyne/azide cycloaddition ("click" chemistry). Properties of the films obtained can be tuned by varying their morphology, their chemically "clicked" content, or by postconstruction functionalization. To demonstrate this, the CV scan rates, component monomers, and "clicked" molecules were varied. Covalent postconstruction immobilization of horseradish peroxidase was also performed. Consequently, pseudocapacitance and enzyme activity were affected. SEEC provides surface scientists an easy access to a wide range of functionalization possibilities in several fields including sensors, fuel cells, photovoltaics, and biomaterials.
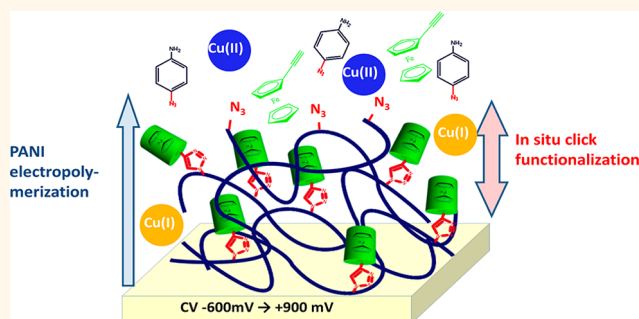
KEYWORDS: nanoscale coating · click chemistry · supercapacitor · polymer · surface sensor · directed assembly

Over the past decade, coating technologies have attracted focused attention from the community of surface scientists. Ideal surface treatments should be rapid, automatable, and highly tolerant to the substrate's nature and topology. The resulting coating should be mechanically and chemically resistant but receptive to a wide range of functionalizations. Until now, the main available strategies, including self-assembly of monolayers (SAM),[1,2] polymer film electropolymerization (EP),[3] and polymer multilayer film deposition (PEM),[4] have failed to fulfill simultaneously these requirements. EP provides yet high-quality coatings, and the inventors of conducting polymers were awarded the 2000 Nobel Prize of Chemistry. EP of polyaniline (PANI) in aqueous mixtures provides robust conducting and industry-friendly polymer matrices without any preliminary synthetic procedures. PANI is one of the most promising conducting polymers due to its simple and inexpensive synthesis.[5−8] The resulting polymer chains are especially prone to self-organize into a variety of supramolecular structures.[9−11] Despite this, functionalizability of PANI films requires optimization, for example, by using the Huisgen Cu(I)-catalyzed cycloaddition, or "click chemistry", where molecules bearing alkyne and azide groups are covalently coupled through stable triazole bonds.[12,13] Clickable SAM,[14,15] PEM,[16,17] and EP[18−20] have been developed, although the multistep process for their assembly and modification does not allow complete control over functionalization. Its spatial resolution control was improved in 2006 with the "electro-click chemistry", where a reductive potential was used to generate catalytic Cu(I) ions from Cu(II).[21−23] This allowed the development of the one-pot "morphogen-driven self-construction" concept where polymer films are built from a solution containing all the building blocks which are reticulated together only when an electric stimulus is

applied by cyclic voltammetry (CV).[24] This unique architecture opens promising avenues of investigation toward immobilization of functional molecules at or within surface coatings.[25−27] However, the highly technical preliminary synthesis of clickable polymers and precoating of the substrate limits its range of applications. Next major developments for coating technology should avoid these pitfalls.

Here, the concept of simultaneous electropolymerization and electro-click functionalization (SEEC) is demonstrated, and the main parameters (which we have termed tuning "levels") for tuning this surface platform are assessed. By using "clickable" electropolymerizable monomers and functional molecules, a CV can be used to polymerize in situ the surface coating and simultaneously functionalize it by electro-click. Films obtained from 4-azidoaniline (ANI-N_3) in conjunction with ethynyl-bearing molecules, using a CV (between −0.6 V and +0.9 V versus Ag/AgCl, scan rate of 50 mV/s), have been particularly studied. This method provides an extremely wide range of surface functionalizations without any synthesis and takes advantage of the intrinsic properties of PANI. Performing SEEC on a mixture of ANI-N_3 and ethynylferrocene (HC≡C-Fc) in the presence of Cu(II) ions leads to both oxidative polymerization of ANI-N_3 and reductive formation of Cu(I) ions, resulting in a continuous growth of functionalized films in one pot (Figure 1). The properties of the obtained coatings are tuned by modifying their morphologies (level 1), changing the clicked molecules (level 2), and postconstruction functionalization (level 3). The potential of SEEC is illustrated by its application for enzyme immobilization and pseudocapacitor design.

RESULTS AND DISCUSSION

Proof of Concept. The validity of the SEEC concept relies on the possibility of both oxidation of ANI-N_3 and reduction of Cu(II) in the same aqueous alcoholic solution using CV. When CV was performed with an ITO electrode in contact with an (ANI-N_3, $CuSO_4$) solution, waves formed upon the reduction of Cu(II) at −0.28 V and oxidation of Cu(s) at +0.2 V and ANI-N_3 at +0.76 V were measured (Supporting Information Figure S-1). When HC≡C-Fc was added to the solution, two wide redox waves emerged at +0.68 and +0.5 V. The poorly defined shape of the peaks clearly indicates that more than one electroactive species are involved. However, both Cu(II) reduction and ANI-N_3 oxidation could be controlled. When CV was performed over longer time periods in the presence of (ANI-N_3, HC≡C-Fc, $CuSO_4$), a polymer film grew continuously on the working electrode whose thickness could be measured by AFM. A minimum average thickness of 180 nm after 100 CV cycles was reached with a corresponding film topology roughness of 110 nm (rms) (Figure 2). When the same solution was used without application of CV, no film deposition was measured and rms reached
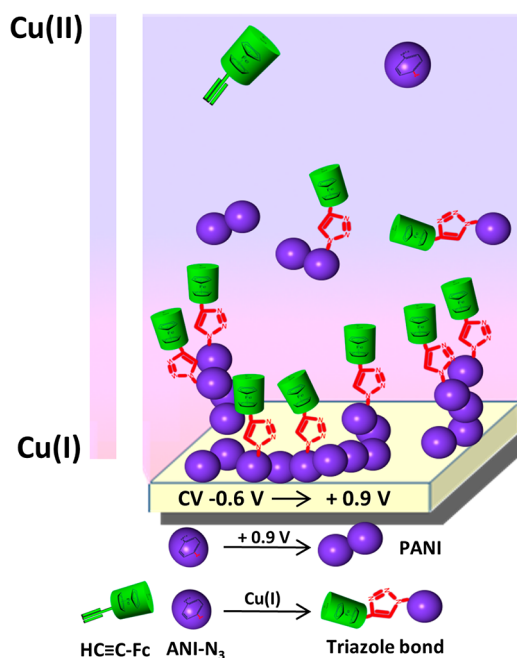

Figure 1. Schematic illustration of the SEEC. Concept is introduced using 4-azidoaniline (ANI-N_3) and ethynylferrocene (HC≡C-Fc) as building blocks in a water/ethanol solution in the presence of Cu(II) ions. Application of a CV between −0.6 V and +0.9 V (vs Ag/AgCl, 50 mV/s) results in both the electropolymerization of the polymer and its electro-click coupling catalyzed by Cu(I),[24] leading to the growth of a functional polymer film.
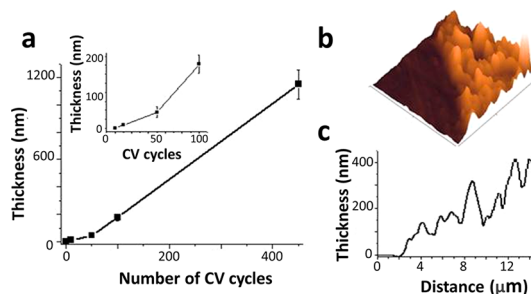
Figure 2. Film growth. (a) Evolution of film thickness during 450 CV cycles (first 100 cycles in inset), measured in the dry state by using AFM in tapping mode, as a function of the number of CV cycles between −0.6 V and +0.9 V (vs Ag/AgCl at a scan rate of 50 mV/s). The film is built up on an ITO electrode in contact with a water/ethanol (50/50 w/w) solution containing 0.5 M H_2SO_4, 10 mM $CuSO_4$, 10 mM ANI-N_3, 10 mM HC≡C-Fc. (b) Three-dimensional AFM height image, obtained in tapping mode and in a dry state, of a $10 \times 10\ \mu m^2$ scratched film area after 100 CV cycles. (c) Corresponding cross-section profile.

9 nm, comparable to the value of a bare ITO electrode (Figure S-2). Electroactive Cu(II) ions and ferrocene groups in the building solution are thus unable to induce ANI-N_3 polymerization by redox reaction at the monomer concentrations used (10 mM), although some reactions have been reported using higher concentrations.[28] Therefore, the applied CV must be the trigger for film formation. UV spectroscopy during the film growth demonstrated a continuous increase of

a

Film morphology

b

c

CV

UV

d
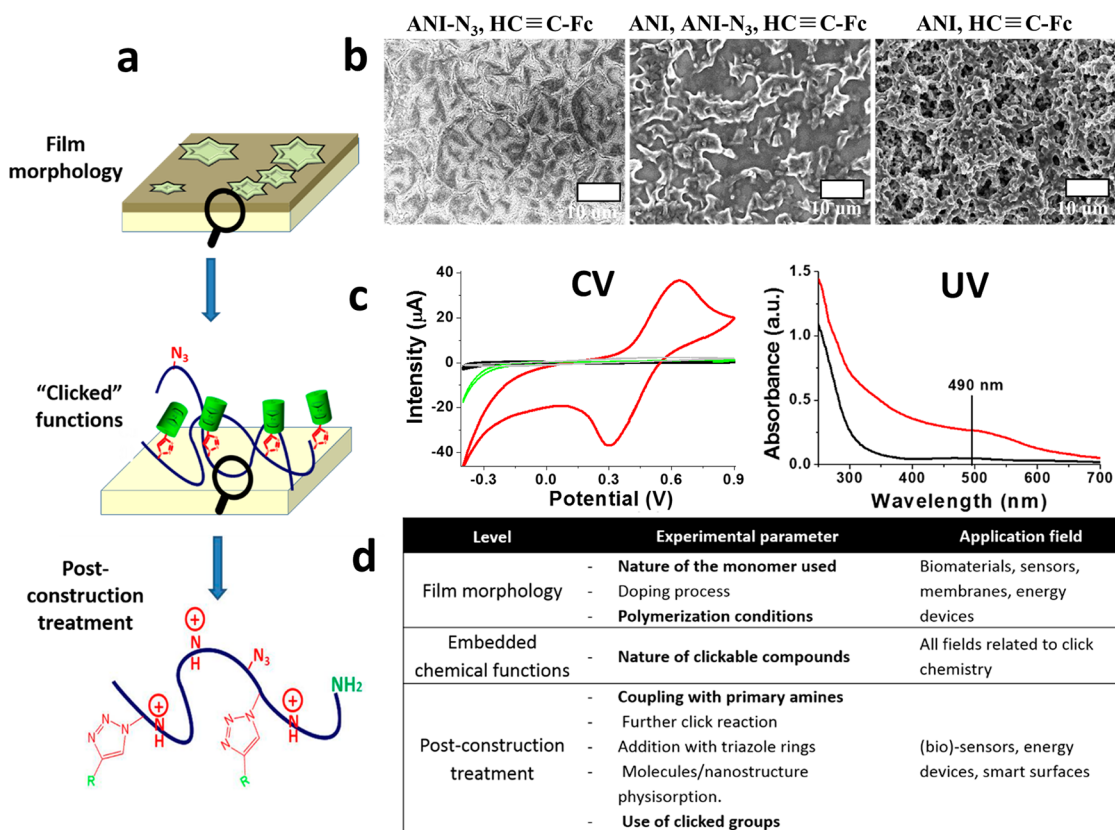
Figure 3. Tuning levels and properties of the film. (a) Schematic representation of the three tuning levels provided by SEEC. **(b)** SEM micrographs at a magnification of 1800× of films obtained after 100 CV cycles from (ANI-N_3, HC≡C-Fc), (ANI, ANI-N_3, HC≡C-Fc) and ANI solutions. The scale bar is 10 μm. **(c, Left)** Typical intensity−potential curves obtained in a 1 M H_2SO_4 solution when a CV from −0.4 V to +0.9 V (scan rate 10 mV/s, reference Ag/AgCl) was applied to a bare ITO substrate (black line) or to a 100 CV cycle film obtained from (ANI-N_3, HC≡C-Fc) with (red line) and without $CuSO_4$ (gray line) or from ANI-N_3 (green line). **(c, Right)** Typical UV spectra of 100 (black line) and 450 (red line) building CV cycle films based on (ANI-N_3, HC≡C-Fc) solutions. **(d)** Summary table of the main tuning levels, experimental parameters, and expected application fields of SEEC applied to PANI films. Parameters written in bold letters are investigated in this article.

absorbance at 490 nm. This indicates a constant deposition of ferrocene, which is the main absorbing species at this wavelength (Figure S-3).

Surprisingly, AFM measurements showed that the film contained only a few void areas after only 10 CV cycles, and the substrate was totally covered after 50 cycles (Figure S-4). After 450 cycles, the film was thick enough to reach the limits of AFM measurement. The surface roughness increased rapidly until 40−100 nm, reaching a plateau after 50 cycles. This morphology is compatible with the polymerization of globular H_2SO_4-doped PANI.[29,30] The mechanism yielding this structure can be attributed to a fast germination process of phenazine aggregates in the first stage of the electropolymerization, acting as a template for PANI propagation.[11]

Characterization of the Film. The SEEC process applied to (ANI-N_3, HC≡C-Fc) solutions was intended to trap covalently ferrocene in the polymer matrix through triazole bonds. Initial evidence for the presence of ferrocene within the film was provided by UV−visible spectroscopy (Figure 3c and Figure S-3). More direct measurements of the coatings were possible using CV for the substrate-bound face of the coating (Figure 3c)

and X-ray photoelectron spectroscopy (XPS) for the top surface (Figure S-5). Intensity−potential signals of films in 1 M H_2SO_4 contain two well-defined redox waves for (ANI-N_3, HC≡C-Fc)-based films. No faradaic current was observed for a bare ITO/PANI-N_3-coated electrode or when the SEEC was applied to an (ANI-N_3, HC≡C-Fc) solution without $CuSO_4$ (Figure 3c). This result suggests trapping of ferrocene by click chemistry close to the electrode. Confirmation of this was obtained from XPS measurements on an (ANI-N_3, HC≡C-Fc) film (Figure S-5). Two peaks corresponding to Fe 2p orbitals at 728 and 712 eV were observed. Analyses from the top surface and substrate-bound faces of the film prove the presence of ferrocene groups, suggesting that functionalization has occurred across the whole polymer matrix. Moreover, XPS atomic ratio analysis suggests a total functionalization reaction with ferrocene as is more fully discussed in the Supporting Information.

The appearance of triazole groups within the film would indicate covalent click immobilization of ferrocene. The XPS signal of the N 1s orbital was compared for films based on ANI, ANI-N_3, and (ANI-N_3, HC≡C-Fc). The presence of nitrogen atoms in the coating obtained

from ANI is indicated by the two peaks at 402 and 399.7 eV. These results correspond to tertiary amine (402 eV) and secondary and primary amines (399.7 eV) and were expected for doped PANI films (Figure S-6a).[31] Nitrogen atoms in coatings based on $ANI-N_3$ gave three peaks at 404.3, 402, and 401 eV. They can, respectively, be attributed to the central electron-deficient nitrogen atoms of azide groups, tertiary amine of aniline, and lateral nitrogen atoms from azide groups.[24] For ($ANI-N_3$, HC≡C-Fc)-based films, the N 1s signal exhibited two peaks at 402 and 400.3 eV. The former is attributed to the tertiary amine of aniline and the heterocyclic 2-nitrogen atoms of triazole groups. The latter corresponds to the lateral 1,3-nitrogen atoms of triazole and primary amines.[24] The emergence of the peak localized at 400.3 eV and disappearance of that at 404.3 eV clearly indicates the formation of triazole groups in the film based on ($ANI-N_3$, HC≡C-Fc). This suggests that all azide groups have been consumed at the top surface of the film. This result is in accordance with XPS atomic ratios and with literature.[24] A full discussion of this topic is available in Supporting Information. However, by using attenuated total reflection infrared spectroscopy (ATR-IR), the presence of azide groups inside ($ANI-N_3$, HC≡C-Fc) films is indicated by the absorption peak at 2120 cm^{-1} (Figure S-7 and Table S-1).[32] ATR-IR spectroscopy also permits assignment of triazole groups in the ($ANI-N_3$, HC≡C-Fc) film, due to the appearance of absorption peaks at 1508 (C−H bending) and 585 cm^{-1} (N−H out of plane), which were absent from the spectra of ANI and $ANI-N_3$-based films. These XPS and ATR-IR data confirm that covalent click immobilization of ferrocene occurs in the film, thus validating the SEEC strategy.

First Level: Morphology Variation. SEEC with aniline derivatives offers three main tuning levels (Figure 3a). The first entails varying the coating morphology, mainly by modifying the film self-construction parameters. Tuning surface roughness can indeed dramatically affect cellular adhesion,[33] electric capacity,[34] or ionic exchange abilities.[35] The effects of the monomer and the CV scan rate used during the buildup were studied.

Electrochemical Conditions. CV scan rate was varied from 100 to 50 then to 10 mV/s. A weak correlation between the film thickness with a decrease in the CV scan rate was found. Yet the growth tendencies were similar, reaching final values of 820 (100 mV/s), 976 (50 mV/s), and 1150 nm (10 mV/s) with standard deviations from 62 to 86 nm (Figure S-8). Differences in film growth mainly originate from the first 100 CV cycles. This growth tendency has to be compared with the corresponding roughness evolution (Figure S-9). For systems using, respectively, 10 and 50 mV/s scan rates, a strong increase of the roughness from 9 nm (bare substrate) to 150 and 110 nm was measured during the first 100 CV cycles, reaching a plateau. At 100 mV/s, the roughness increase is less significant

with a maximum value of 32 nm. The decoupling between the different film growths for different scan rates coincided with the decoupling of the corresponding rms values. Larger aggregates seem to be deposited at slower CV scan rates, leading to both thicker and rougher coatings (Figures S-8 and S-9). This may originate from the division of the oxidation periods of $ANI-N_3$ and of the reduction of Cu(II) when the CV scan rate is increased. As a consequence, the reaction time of electrogenerated species is limited, restricting the molecular nucleation of globules and their supramolecular aggregation.[36]

Variation of Monomers. The surface morphology was also strongly affected by the nature of the ANI derivative monomer used.[11] Indeed, the use of substituted anilines may affect the structure of the polymer chain and its supramolecular organization. This parameter was investigated by using either pure $ANI-N_3$, an equimolar solution of $ANI-N_3$ and ANI, and pure ANI as monomers. An ATR-IR study of the resulting films confirmed the inclusion of both $ANI-N_3$ and ANI in the (ANI, $ANI-N_3$, HC≡C-Fc) system with peaks corresponding to azide, triazole, and polyaniline sulfate (1390−1490, 550−570 cm^{-1}) (Figure S-10 and Table S-2). SEM observations of the different coating types after 100 CV cycles are shown on Figure 3b. After 100 CV cycles, ($ANI-N_3$, HC≡C-Fc)-based films were characterized by a flat and wrinkled morphology (magnification of 1800×) containing a porous structure at higher magnifications (Figure S-12). After increased numbers of CV cycles, the same structure was obtained with a densification of the porous network, in accordance with the roughness plateau obtained from AFM data (Figures S-11 and S-12). The ANI-based system displayed a rough morphology with a mix of globular and globular-melted structures at low and high magnifications (Figures 3b and S-13). However, after 450 cycles, nanoscale rods at the surface of the polymer network could be observed (Figures S-11 and S-13). (ANI, $ANI-N_3$, HC≡C-Fc)-based films showed an intermediate morphology with star-shaped aggregated domains alternating with flat areas (Figure 3b). After 450 cycles, this changed to a rough globular-like morphology. However, at higher magnifications, fibers could be observed both after 100 and 450 cycles (Figures S-11 and S-14). Appearance of fibers in (ANI, $ANI-N_3$, HC≡C-Fc) films may affect their charge transport properties.[37] An initial study of the electrical characteristics of the coating was provided by the intensity−potential signal measured during its buildup. When ($ANI-N_3$, HC≡C-Fc) was used, the current intensity decreased with the number of CV cycles (Figure S-15). With (ANI, $ANI-N_3$, HC≡C-Fc), the intensity decreased during the first 50 cycles then increased to 5 times the initial intensity. ANI addition to ($ANI-N_3$, HC≡C-Fc) building solutions increases the coating conductivity due to the formation of either a copolymer or an interpenetrated double network, in accordance with SEM data.
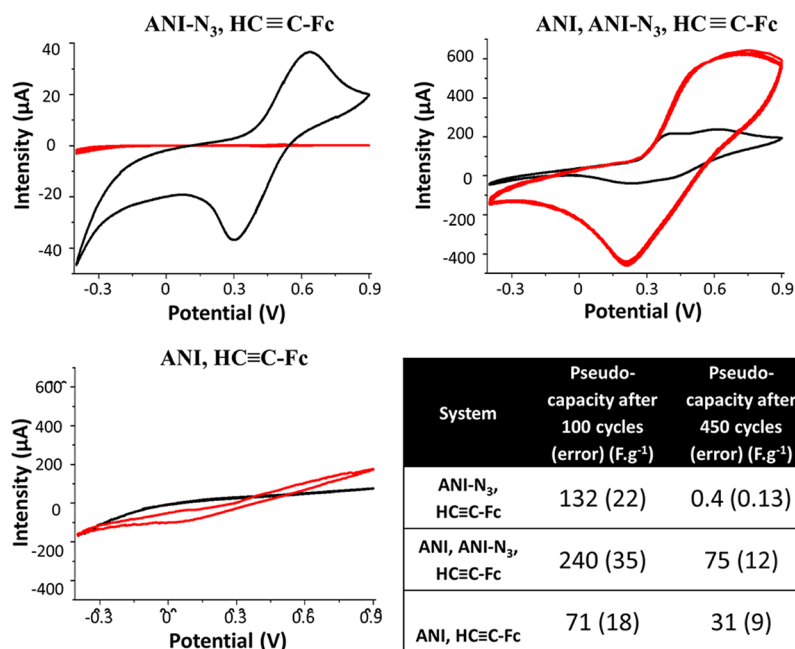
Figure 4. Influence of the monomer and clicked molecules over the film electrical pseudocapacitance. CV intensity−potential curves, obtained using a 10 mV/s scan rate (reference Ag/AgCl) in 1 M H_2SO_4, of (ANI-N_3, Fc-C), (ANI, ANI-N_3, Fc-C), and ANI films after 100 (black line) or 450 (red line) building cycles. Summary table of the corresponding calculated electrical pseudocapacitances.

Far from being restricted to ANI-N_3-based films, the SEEC process can be performed using other electro-polymerizable monomers such as 4-ethynylaniline (HC≡C-ANI) or 2-ethynyl-6-methoxynaphthalene (HC≡C-naphthalene) combined with poly(ethylene glycol)methyl ether azide (PEG-N_3). The corresponding films exhibited either a fiber or granular morphology (Figure S-16). ATR-IR studies confirmed the click immobilization of PEG-N_3 in the HC≡C-ANI- (Figure S-17) and HC≡C-naphthalene-based (Figure S-18) matrices.

Electrical Pseudocapacitance Properties of the Films. The SEEC process allows an easy tuning of the coating, as demonstrated by the various morphologies obtained. Yet these chemical and morphological changes are expected to result in new film properties. For this reason, the specific case of the coating's electrical pseudocapacitance has been studied. Conductive polyaniline films are known to be excellent pseudo-capacitance platforms whose performances are critically influenced by the coating morphology and immobilized electroactive molecules.[11] Chemical immobilization of new redox centers like ferrocene within the film may improve performances.[38]

The pseudocapacitive currents of (ANI-N_3, HC≡C-Fc)-, (ANI, ANI-N_3, HC≡C-Fc)-, and (ANI, HC≡C-Fc)-based films were measured (Figure 4). In accordance with the CV buildup data, the values for (ANI-N_3, HC≡C-Fc) were much higher for thinner films. The presence of ferrocene within the polymer matrix resulted in the film attaining a specific pseudocapacitance value of around 130 F g^{-1} for thin films *versus* less than 1 F g^{-1} for thicker films. Substituted aniline exhibits a weaker conductivity than

aniline because it undergoes side reactions limiting both the conjugation of the polymer backbone and the film crystallinity.[39] For (ANI, ANI-N_3, HC≡C-Fc) coatings, the current increases with the film thickness. The specific pseudocapacitance reached a maximum (240 F g^{-1}) for 100 CV cycle films (Figure 4). This result may be explained by the better accessibility of redox centers in the thinner coatings even if the deposited material is conductive: an ideal (pseudo)capacitor needs a fast charge transfer.[34] The same phenomenon was observed with the (ANI, HC≡C-Fc) system, but the absence of trapped ferrocene limited the pseudocapacitance. The presence of both ANI and clicked ferrocene in the polymer matrix induced a dramatic increase in pseudocapacitance performance, indicating the synergistic effect provided by SEEC.

Second Level: Variation of Clickable Groups. The SEEC process takes advantage of the wide range and growing library of molecules available for click chemistry leading to numerous functionalization possibilities.[40,41] We defined this ability as the second tuning level (Figure 3a,d). As examples, other clickable molecules, namely, undecynoic acid (HC≡C-COOH), ethynyl-benzaldehyde (HC≡C-Bz-CHO), and phenylacetylene (HC≡C-Ph), were used instead of HC≡C-Fc. ATR-IR spectra of (ANI-N_3, HC≡C-COOH), (ANI-N_3, HC≡C-Fc), (ANI-N_3, HC≡C-Ph), and (ANI-N_3, HC≡C-Bz-CHO) films all exhibited peaks localized at 2120 (azide),[32] 1508 (triazole C−H bending), and 585 cm^{-1} (triazole N−H out of plane),[42] demonstrating that the click reaction had occurred (Figures 5a,b and S-19 and Table S-3). Evidence for the presence of undecynoic acid in (ANI-N_3, HC≡C-COOH)-based films is provided by the stronger
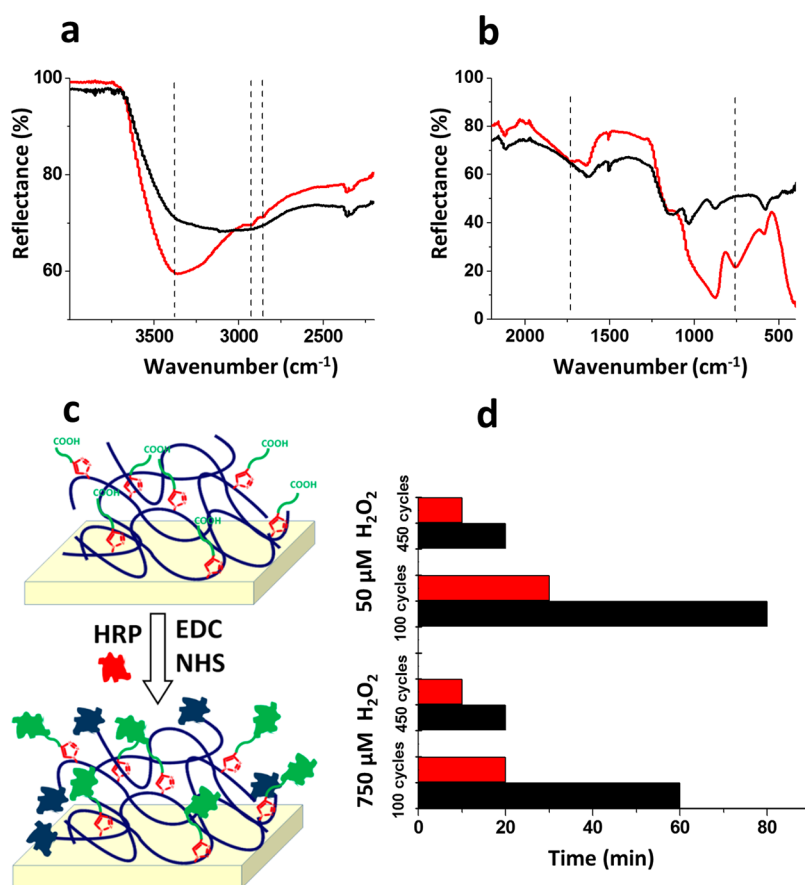
Figure 5. Postconstruction functionalization of the film. Typical ATR-IR reflectance spectra, in the 4000−2200 (a) and the 2200−400 (b) regions, of films obtained by CV treatment of (ANI-N$_3$, HC≡C-Fc) (black line) and (ANI-N$_3$, HC≡C-COOH) (red line) solutions. Dashed lines identify the main peaks due to undecynoic acid. Complete peak assignment is presented in Table S-3. (c) Schematic representation of a (ANI-N$_3$, HC≡C-COOH)-based film postconstruction functionalization with horseradish peroxidase (HRP) using the EDC/NHS approach. Free (red) HRP is depicted as green when covalently coupled to carboxylic acid functions and black when bound with chain terminal primary amines. (d) Time (min) needed to reach the maximum conversion of substrate to quinoneimine product in the solutions with initial H$_2$O$_2$ concentration of 50 and 750 μM, brought to contact with HRP functionalized films obtained from ANI-N$_3$ (black) or (ANI-N$_3$, HC≡C-COOH) (red) after 100 and 450 CV building cycles.

absorption around 3300 cm^{-1} (O−H stretching), two small absorption peaks due to aliphatic C−H$_2$ stretching (2850 and 2930 cm^{-1}), and the carboxylic C═O stretching peak (1720 cm^{-1}). When HC≡C-Bz-CHO was used, the SEEC conditions (CV, acidic solution) reduced the aldehyde function into alcohol (1080 cm^{-1}). Therefore, click reticulation of various ethynyl-containing molecules into the polymer matrix by SEEC was confirmed.

Third Level: Postconstruction Functionalization. The third main tuning level for SEEC consists of postconstruction functionalization (Figure 3a,d). Amines, aromatic rings, remaining azides, and newly added "clicked" functionalities provide potentially orthogonal chemical modification methods. Additional adsorption of charged molecules and nanostructures can also be achieved, owing to the positive charge of polymerized aniline in acidic media. To investigate this level, ANI-N$_3$ and (ANI-N$_3$, HC≡C-COOH)-based films were used for chemical postconstruction immobilization of horseradish peroxidase (HRP). 1-Ethyl-3-(3-(dimethylamino)propyl)carbodiimide (EDC) and N-hydroxysuccinimide (NHS) activators, which

induce covalent coupling between carboxylic and primary amine groups, have recently been used to modify end-chain primary amines of polyaniline.[43,44] Introduction of carboxyl groups into the film by the SEEC process allows increases in the coating immobilization capability due to enzyme coupling to both primary amine and carboxyl groups as depicted in Figure 5c.

HRP was immobilized on ANI-N$_3$ and (ANI-N$_3$, HC≡C-COOH) films after either 100 or 450 CV cycles. The modified coatings were tested for their HRP activity by following the formation of quinoneimine by UV−visible absorbance at 505 nm (see details in the Materials section). Films based on (ANI-N$_3$, HC≡C-COOH) exhibited systematically a faster response than ANI-N$_3$ coatings to H$_2$O$_2$ (Figure 5d). This improvement suggests that the number or the activity of bound HRP is increased in (ANI-N$_3$, HC≡C-COOH) films. Moreover, the conversion performances were systematically higher when thicker films were used, indicating enzyme immobilization at the surface and interior of the coatings. For 100 CV cycles films, increasing the H$_2$O$_2$ concentration resulted

in shorter conversion times, indicating that, for these films, the enzyme is not saturated with substrate at 50 μM H_2O_2 yet. For thicker films, the activity of immobilized enzymes appeared high enough to fully form the dye within 10 and 20 min. The third film tuning level of SEEC was thus demonstrated, using both intrinsic primary amine groups of PANI and carboxyl groups added during the film buildup.

CONCLUSION

Simultaneous electropolymerization and electro-click functionalization (SEEC) has been demonstrated using ethynylferrocene (HC≡C-Fc) as a reactant for the click functionalization. The process is simple and quick and does not involve any preliminary synthesis. A continuous increase of the film thickness with the number of CV cycles was found up to 450 cycles. Coatings obtained by SEEC provide outstanding tuning possibilities through three main levels: controlling the film morphology, varying the "clickable" functional molecules and monomers, and performing postconstruction treatments. As a proof of concept, each level has been investigated by changing either the electropolymerization conditions or the monomer structure (first level), varying the clicked molecules (second level), and performing a postconstruction treatment (third level). Using the first level, it was demonstrated that films of various chemical composition, with globular, fibrous, and flat porous morphologies could be obtained, exhibiting different electrical pseudocapacitances. The second and third levels allowed the introduction of carboxylic functions in the matrix and their successful use for enzyme immobilization. This work provides an insight into the interplay between the different functionalization levels of SEEC which should rapidly lead to applications in fields as diverse as sensors, membranes, fuel/energetic devices, biomaterials, or stimuli-responsive coatings.

METHODS

Materials. 4-Azidoaniline (ANI-N_3, M = 170.6 g/mol, CAS 91159-79-4), 4-ethynylaniline (ANI-C≡CH, M = 117.1 g/mol, CAS 14235-81-5), ethynylferrocene (HC≡C-Fc, M = 210.1 g/mol, CAS 1271-47-2), 10-undecynoic acid (HC≡C-COOH, M = 182.3 g/mol, CAS 2777-65-3), 2-ethynyl-6-methoxynaphthalene (HC≡C-naphthalene, M = 182.2 g/mol, CAS 129113-00-4), N-hydroxysuccinimide (NHS, M = 115.1 g/mol, CAS 6066-82-6), poly(ethylene glycol)methyl ether azide (PEG-N_3, M_n = 1000, CAS 89485-61-0), and copper sulfate pentahydrate (CuSO$_4$·5H$_2$O, M = 249.7 g/mol, CAS 7758-99-8) were purchased from Sigma-Aldrich. Aniline (ANI, M = 93.1 g/mol, CAS 62-53-3), horseradish peroxidase (HRP, 100 units/mg, CAS 9003-99-0), copper(II) chloride (M = 134.4 g/mol, CAS 7447-39-4), and hydrogen peroxide (H_2O_2, 30%, M = 34.0 g/mol, CAS 7722-84-1) were purchased from Wako. 1-Ethyl-3-(3-(dimethylamino)propyl)carbodiimide hydrochloride (EDC, M = 191.7 g/mol, CAS 25952-53-8), 4-aminoantipyrine (4-AA, M = 203.2 g/mol, CAS 83-07-8), phenylacetylene (M = 94.1 g/mol, CAS 536-74-3), and phenol (M = 94.1 g/mol, CAS 108-95-2) were purchased from Nacalai Tesque. 4-Ethynylbenzaldehyde (HC≡C-benzaldehyde, M = 130.1 g/mol, CAS 63697-96-1) was purchased from AK Scientific Inc.

Preparation of ANI Solutions. All solutions were prepared using absolute ethanol (VWR, 99.5% purity) and Milli-Q water (18.2 MΩ cm^{-1}) purified using a Purelab Prima system. The reactants were prepared in separated solutions and freshly mixed before use. All solutions were based on a 50/50 (v/v) water/ethanol mixture in the presence of 10 mM CuSO$_4$ and 0.5 M H_2SO_4. All solutions of ANI, ANI-N_3, and the mixtures (ANI-N_3, HC≡C-Fc), (ANI-N_3, HC≡C-COOH), and (ANI, ANI-N_3, HC≡C-Fc) contained 10 mM of the respective aniline derivative and 10 mM of the respective ethynyl-bearing molecules (if any). Hydrophobic molecules were first dissolved in ethanol.

Cyclic Voltammetry (CV). A CHI model 613B potentiostat was used with three-electrode apparatus based on an ITO-coated quartz (area 2.16 cm^2) as working electrode, a platinum wire as counter electrode, and an RE1S Ag/AgCl-based reference electrode. The electrodes were purchased from ALS.

Film Buildup Procedure and Characterization. SEEC with HC≡C-naphthalene was performed by CV (between −600 mV and +1500 mV, scan rate of 100 mV/s) applied to an ITO substrate in contact with a solution containing 10 mM CuCl$_2$, 0.5 M HCl, 10 mM HC≡C-naphthalene, and 5 mM PEG-N_3.

SEEC with ANI-based monomers was performed using a CV operating between −600 mV and +900 mV (scan rates of 10, 50, and 100 mV/s) applied to an ITO substrate in contact with the building solutions. After construction, the capacitive current was measured using CV between −400 mV and +900 mV in 1 M H_2SO_4 at 10 mV/s. The global specific film capacity was calculated for a potential range between −400 mV and +900 mV according to the following equation:[45]

$$C_s = \frac{1}{2.6 \times m \times s} \times \left[\int_{-0.4}^{0.9} I(E) \times dE - \int_{0.9}^{-0.4} I(E) \times dE \right] \quad (1)$$

where C_s is the specific capacity, m the coating mass, s the scan rate of the CV, $I(E)$ the current intensity, and E the electric potential. The mass of the coated electrode was measured after drying overnight at 50 °C.

Postconstruction Functionalization. Following the SEEC process, the electrode was placed in contact with a solution containing 15 mM EDC and 30 mM NHS for 1 h, rinsed, and dipped in a 20 mM phosphate buffer solution containing 100 U/mL HRP. The functionalized electrode was stored at 5 °C.

Peroxidase Activity Assay. The activity of HRP was evaluated by monitoring the UV/vis spectrophotometry appearance of the quinone−imine dye formed upon oxidative coupling of 4-aminoantipyrine and phenol (eq 2).

$$2H_2O_2 + 4\text{-AA} + \text{phenol} \longrightarrow \text{quinoneimine dye} + 4H_2O \quad (2)$$
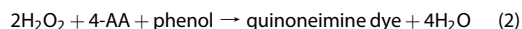
The product conversion by immobilized HRP was determined by immersing functionalized films in phosphate buffer solution (50 mM, pH 6) of 2 mM 4-AA, 21 mM phenol, and 50−750 μM H_2O_2. Absorbance at 505 nm was measured every 10 min for 90 min and subsequently every hour. The maximum absorbance was measured after dissolving HRP in the probing solution at excess concentration (5 mg/mL) ensuring fast and complete substrate conversion. The conversion rate was then calculated using the following (eq 3):

$$C\,(\%) = \frac{A_t - A_{t_0}}{A_{max} - A_{t_0}} \times 100 \quad (3)$$

where A_t is the absorbance of the solution in contact with the film at time t, A_{t_0} the initial absorbance of the solution before contact with the film, and A_{max} the absorbance measured when HRP was directly dissolved in the solution.

Atomic Force Microscopy. The images were obtained by using an AFM SPA400-SPI4000 (Seiko Instruments Inc., Chiba, Japan) in tapping mode at optimal force and in dried state. Height images were scanned at a fixed scan rate (0.3 Hz). Data evaluation was

performed using the Gwyddion software. Film thicknesses were determined by imaging films after scratching. The minimum average thicknesses of the scratched films were determined by measuring at least three different areas of three different samples.

Scanning Electron Microscopy. SEM was performed using a Hitachi S-4800 at acceleration voltages of 10 kV. The samples were observed directly after 15 min drying under vacuum.

UV−Visible Spectroscopy. A Shimadzu UV−visible NIR spectrophotometer (model UV-3600) was used to study the (ANI-N_3, HC≡C-Fc) system and the product of peroxidase activity assay. Absorbance at 490 nm, allowing detection of ferrocene groups, was measured during the buildup.

Attenuated Total Reflection Infrared Spectroscopy. ATR-IR was performed on ANI, ANI-N_3, (ANI-N_3, HC≡C-Fc), (ANI, ANI-N_3, HC≡C-Fc), and (ANI-N_3, HC≡C-COOH)-based films using a Thermoscientifique Nicolet 4700 apparatus.

X-ray Photoelectron Spectroscopy. XPS was carried out on an ESCALAB Mark II (VG Company, U.K.).

Conflict of Interest: The authors declare no competing financial interest.

Supporting Information Available: Control experiments, CV and UV−vis measurements during the buildup, chemical analysis by XPS and ATR-IR spectroscopies, as well as characterization of the coating topography by AFM and SEM. This material is available free of charge *via* the Internet at http://pubs.acs.org.

REFERENCES AND NOTES

1. Bain, C.; Whitesides, G. Molecular-Level Control over Surface Order in Self-Assembled Monolayer Films of Thiols on Gold. *Science* **1988**, *240*, 62–63.
2. Rubinstein, I.; Steinberg, S.; Tor, Y.; Shanzer, A.; Sagiv, J. Ionic Recognition and Selective Response in Self-Assembling Monolayer Membranes on Electrodes. *Nature* **1988**, *332*, 426–429.
3. MacDiarmid, A. G. "Synthetic Metals": A Novel Role for Organic Polymers (Nobel Lecture). *Angew. Chem., Int. Ed.* **2001**, *40*, 2581–2590.
4. Decher, G. Fuzzy Nanoassemblies: Toward Layered Polymeric Multicomposites. *Science* **1997**, *277*, 1232–1237.
5. Lee, K.; Cho, S.; Heum Park, S.; Heeger, A. J.; Lee, C.-W.; Lee, S.-H. Metallic Transport in Polyaniline. *Nature* **2006**, *441*, 65–68.
6. Gustafsson, G.; Cao, Y.; Treacy, G. M.; Klavetter, F.; Colaneri, N.; Heeger, A. J. Flexible Light-Emitting Diodes Made from Soluble Conducting Polymers. *Nature* **1992**, *357*, 477–479.
7. Anderson, M.; Mattes, B.; Reiss, H.; Kaner, R. Conjugated Polymer-Films for Gas Separations. *Science* **1991**, *252*, 1412–1415.
8. Scott, C. L.; Pumera, M. Carbon Nanotubes Can Exhibit Negative Effects in Electroanalysis due to Presence of Nanographite Impurities. *Electrochem. Commun.* **2011**, *13*, 426–428.
9. Ciric-Marjanovic, G. Recent Advances in Polyaniline Research: Polymerization Mechanisms, Structural Aspects, Properties and Applications. *Synth. Met.* **2013**, *177*, 1–47.
10. Ciric-Marjanovic, G. Recent Advances in Polyaniline Composites with Metals, Metalloids and Nonmetals. *Synth. Met.* **2013**, *170*, 31–56.
11. Sapurina, I. Y.; Shishov, M. A. Oxidative Polymerization of Aniline: Molecular Synthesis of Polyaniline and the Formation of Supramolecular Structures. In *New Polymers for Special Applications*; De Souza Gomes, A., Ed.; InTech: Winchester, U.K., 2012.
12. Tornøe, C. W.; Christensen, C.; Meldal, M. Peptidotriazoles on Solid Phase: [1,2,3]-Triazoles by Regiospecific Copper(I)-Catalyzed 1,3-Dipolar Cycloadditions of Terminal Alkynes to Azides. *J. Org. Chem.* **2002**, *67*, 3057–3064.
13. Rostovtsev, V. V.; Green, L. G.; Fokin, V. V.; Sharpless, K. B. A Stepwise Huisgen Cycloaddition Process: Copper(I)-Catalyzed Regioselective "Ligation" of Azides and Terminal Alkynes. *Angew. Chem.* **2002**, *114*, 2708–2711.
14. Toulemon, D.; Pichon, B. P.; Leuvrey, C.; Zafeiratos, S.; Papaefthimiou, V.; Cattoen, X.; Begin-Colin, S. Fast Assembling of Magnetic Iron Oxide Nanoparticles by Microwave-Assisted Copper(I) Catalyzed Alkyne-Azide Cycloaddition (CuAAC). *Chem. Mater.* **2013**, *25*, 2849–2854.
15. Zhang, Y.; Luo, S. Z.; Tang, Y. J.; Yu, L.; Hou, K. Y.; Cheng, J. P.; Zeng, X. Q.; Wang, P. G. Carbohydrate-Protein Interactions by "Clicked" Carbohydrate Self-Assembled Monolayers. *Anal. Chem.* **2006**, *78*, 2001–2008.
16. Such, G. K.; Quinn, J. F.; Quinn, A.; Tjipto, E.; Caruso, F. Assembly of Ultrathin Polymer Multilayer Films by Click Chemistry. *J. Am. Chem. Soc.* **2006**, *128*, 9318–9319.
17. Rydzek, G.; Schaaf, P.; Voegel, J.-C.; Jierry, L.; Boulmedais, F. Strategies for Covalently Reticulated Polymer Multilayers. *Soft Matter* **2012**, *8*, 9738–9755.
18. Cernat, A.; Griveau, S.; Martin, P.; Lacroix, J. C.; Farcau, C.; Sandulescu, R.; Bedioui, F. Electrografted Nanostructured Platforms for Click Chemistry. *Electrochem. Commun.* **2012**, *23*, 141–144.
19. Inagi, S.; Fuchigami, T. Electrochemical Post-functionalization of Conducting Polymers. *Macromol. Rapid Commun.* **2014**, 10.1002/marc.201400023.
20. Shida, N.; Ishiguro, Y.; Atobe, M.; Fuchigami, T.; Inagi, S. Electro-Click Modification of Conducting Polymer Surface Using Cu(I) Species Generated on a Bipolar Electrode in a Gradient Manner. *ACS Macro Lett.* **2012**, *1*, 656–659.
21. Devaraj, N. K.; Dinolfo, P. H.; Chidsey, C. E. D.; Collman, J. P. Selective Functionalization of Independently Addressed Microelectrodes by Electrochemical Activation and Deactivation of a Coupling Catalyst. *J. Am. Chem. Soc.* **2006**, *128*, 1794–1795.
22. Rydzek, G.; Thomann, J.-S.; Ben Ameur, N.; Jierry, L.; Mésini, P.; Ponche, A.; Contal, C.; El Haitami, A. E.; Voegel, J.-C.; Senger, B.; *et al.* Polymer Multilayer Films Obtained by Electrochemically Catalyzed Click Chemistry. *Langmuir* **2010**, *26*, 2816–2824.
23. Ku, S.-Y.; Wong, K.-T.; Bard, A. J. Surface Patterning with Fluorescent Molecules Using Click Chemistry Directed by Scanning Electrochemical Microscopy. *J. Am. Chem. Soc.* **2008**, *130*, 2392–2393.
24. Rydzek, G.; Jierry, L.; Parat, A.; Thomann, J.-S.; Voegel, J.-C.; Senger, B.; Hemmerle, J.; Ponche, A.; Frisch, B.; Schaaf, P.; *et al.* Electrochemically Triggered Assembly of Films: A One-Pot Morphogen-Driven Buildup. *Angew. Chem., Int. Ed.* **2011**, *50*, 4374–4377.
25. Rydzek, G.; Polavarapu, P.; Rios, C.; Tisserant, J.-N.; Voegel, J.-C.; Senger, B.; Lavalle, P.; Frisch, B.; Schaaf, P.; Boulmedais, F. *et al.* Morphogen-Driven Self-Construction of Covalent Films Built from Polyelectrolytes and Homobifunctional Spacers: Buildup and pH Response. *Soft Matter* **2012**, *8*, 10336–10343.
26. Rydzek, G.; Parat, A.; Polavarapu, P.; Baehr, C.; Voegel, J.-C.; Hemmerle, J.; Senger, B.; Frisch, B.; Schaaf, P.; Jierry, L.; *et al.* One-Pot Morphogen Driven Self-Constructing Films Based on Non-covalent Host−Guest Interactions. *Soft Matter* **2012**, *8*, 446–453.
27. Rydzek, G.; Garnier, T.; Schaaf, P.; Voegel, J.-C.; Senger, B.; Frisch, B.; Haikel, Y.; Petit, C.; Schlatter, G.; Jierry, L.; *et al.* Self-Construction of Supramolecular Polyrotaxane Films by an Electrotriggered Morphogen-Driven Process. *Langmuir* **2013**, *29*, 10776–10784.
28. Guo, X.; Fei, G. T.; Su, H.; Zhang, L. D. Synthesis of Polyaniline Micro/Nanospheres by a Copper(II)-Catalyzed Self-Assembly Method with Superior Adsorption Capacity of Organic Dye from Aqueous Solution. *J. Mater. Chem.* **2011**, *21*, 8618–8625.
29. Stejskal, J.; Sapurina, I.; Trchová, M.; Konyushenko, E. N. Oxidation of Aniline: Polyaniline Granules, Nanotubes, and Oligoaniline Microspheres. *Macromolecules* **2008**, *41*, 3530–3536.
30. Shishov, M. A.; Moshnikov, V. A.; Sapurina, I. Y. Self-Organization of Polyaniline during Oxidative Polymerization: Formation of Granular Structure. *Chem. Pap.* **2013**, *67*, 909–918.

31. Yue, J.; Epstein, A. XPS Study of Self-Doped Conducting Polyaniline and Parent Systems. *Macromolecules* **1991**, *24*, 4441–4445.

32. Palomaki, P. K. B.; Dinolfo, P. H. Structural Analysis of Porphyrin Multilayer Films on ITO Assembled Using Copper(I)-Catalyzed Azide−Alkyne Cycloaddition by ATR IR. *ACS Appl. Mater. Interfaces* **2011**, *3*, 4703–4713.

33. Kriparamanan, R.; Aswath, P.; Zhou, A.; Tang, L.; Nguyen, K. T. Nanotopography: Cellular Responses to Nanostructured Materials. *J. Nanosci. Nanotechnol.* **2006**, *6*, 1905–1919.

34. Simon, P.; Gogotsi, Y. Materials for Electrochemical Capacitors. *Nat. Mater.* **2008**, *7*, 845–854.

35. Kim, S. Y.; Kim, S.; Park, M. J. Enhanced Proton Transport in Nanostructured Polymer Electrolyte/ionic Liquid Membranes under Water-Free Conditions. *Nat. Commun.* **2010**, *1*, 88.

36. Huang, J. X.; Kaner, R. B. The Intrinsic Nanofibrillar Morphology of Polyaniline. *Chem. Commun.* **2006**, 367–376.

37. Zhang, Y.; Jiang, X.; Zhang, R.; Sun, P.; Zhou, Y. Influence of the Nanostructure on Charge Transport in Polyaniline Films. *Electrochim. Acta* **2011**, *56*, 3264–3269.

38. Fabre, B. Ferrocene-Terminated Monolayers Covalently Bound to Hydrogen-Terminated Silicon Surfaces. Toward the Development of Charge Storage and Communication Devices. *Acc. Chem. Res.* **2010**, *43*, 1509–1518.

39. Jadhav, A. V.; Gulgas, C. G.; Gudmundsdottir, A. D. Synthesis and Properties of Poly(aniline-*co*-azidoaniline). *Eur. Polym. J.* **2007**, *43*, 2594–2603.

40. Lutz, J.-F.; Zarafshani, Z. Efficient Construction of Therapeutics, Bioconjugates, Biomaterials and Bioactive Surfaces Using Azide-Alkyne "Click" Chemistry. *Adv. Drug Delivery Rev.* **2008**, *60*, 958–970.

41. Meldal, M. Polymer "Clicking" by CuAAC Reactions. *Macromol. Rapid Commun.* **2008**, *29*, 1016–1051.

42. El-Azhary, A. A.; Suter, H. U.; Kubelka, J. Experimental and Theoretical Investigation of the Geometry and Vibrational Frequencies of 1,2,3-Triazole, 1,2,4-Triazole, and Tetrazole Anions. *J. Phys. Chem. A* **1998**, *102*, 620–629.

43. Girardot, J. M. D.; Girardot, M. N. Amide Cross-Linking: An Alternative to Glutaraldehyde Fixation. *J. Heart Valve Dis.* **1996**, *5*, 518–525.

44. Lee, J. M.; Edwards, H. H. L.; Pereira, C. A.; Samii, S. I. Crosslinking of Tissue-Derived Biomaterials in 1-Ethyl-3-(3-dimethylaminopropyl)-carbodiimide (EDC). *J. Mater. Sci.: Mater. Med.* **1996**, *7*, 531–541.

45. Khomenko, V.; Frackowiak, E.; Béguin, F. Determination of the Specific Capacitance of Conducting Polymer/Nanotubes Composite Electrodes Using Different Cell Configurations. *Electrochim. Acta* **2005**, *50*, 2499–2506.